Supported membranes on chemically structured and rough surfaces

Peter S. Swain

Center for Studies in Physics and Biology, The Rockefeller University, 1230 York Avenue, New York, New York 10021

David Andelman

*School of Physics and Astronomy, Raymond and Beverly Sackler Faculty of Exact Sciences, Tel Aviv University,
Ramat Aviv 69978, Tel Aviv, Israel*

We present a general linear response description of membrane adhesion at rough or chemically structured surfaces. Our method accounts for nonlocal Van der Waals effects and contains the more approximate (and local) Deryagin approach in a simple limit. Specializing to supported membranes we consider the effects of substrate structure on the membrane adhesion energy and configuration. Adhesion is usually less favorable for rough substrates and the membrane shape tends to follow that of the surface contours. Chemical patterning (described by a spatially varying Van der Waals force), however, favors adhesion with the membrane configuration being out of phase with the surface structure. Finally, considering a surface indented with ''V''-shaped trenches, we show that our approach is in good agreement with an exact numerical solution.

I. INTRODUCTION

Supported membranes strongly adhere to substrates and lie typically at separation distances of between 10 and 40 Å [1]. Such small values have lead to their adoption by the biotechnology industry [2] and, in particular, given them an important role in the development of biosensors. Supported membranes enable one to biofunctionalize an inorganic surface and can provide an ultrathin, highly electrically resistant layer on top of a conducting substrate. They provide a means of immobilizing proteins with a well-defined orientation and in a nondenaturing environment [3]. If these proteins are receptors then one can use electrical or optical means to detect or ''sense'' the binding of ligands to the receptors [4].

Supported membranes can be formed by the spreading of a bilayer over a substrate, vesicle fusion taking place at a substrate or by lipid monolayer transfer using a Langmuir-Blodgett technique [1]. However, in nearly all applications the substrates used are not simply planar and homogeneous but are patterned, either chemically [4,5] or geometrically [6,7]. The theory of membrane adhesion has typically concentrated on adhesion at ideal planar surfaces [8]. In a recent paper [9], we have provided a simple description of the adhesive properties of membranes at rough surfaces. In this article, we would like to present a more general approach to membrane adhesion which includes the possibilities of chemical patterning and surface roughness. Both cases are modeled making use of a position dependent Van der Waals force.

We begin with a summary of the basic assumptions of our model and of the intermolecular interactions involved. In Sec. III, a planar, homogeneous substrate is considered as the starting point for the linear response theory that follows. We show in Secs. IV and V how the simpler approach of Ref. [9] is included in the present work and then proceed to consider several illustrative examples in Sec. VI. Finally in Sec. VII, our analytical description is compared and contrasted with a complete numerical solution. Throughout, we emphasize the effect of substrate roughness and chemical heterogeneities on the adhesive properties of the supported membrane.

II. THE FREE ENERGY

To begin we consider a membrane supported at a substrate that can be either geometrically structured (nonplanar), Fig. 1(a), or chemically structured (patterned with different chemical compounds), Figs. 1(b) and 1(c). For example, a surface can be chemically structured by depositing different chemical layers, see Fig. 1(b), or adjoining different chemical surfaces together to make a columnar structure, Fig. 1(c). Both of these can be described by a spatially variant Van der Waals force and it is this particular chemical structure which we specialize to. For a membrane adhering to such a surface this patterning will greatly influence the membrane configuration and adhesion energy. Inspired by advances in the theory of wetting [10], we adopt a general mean-field approach in which the configuration taken up by the membrane is one that minimizes the free energy. In order to find this optimum configuration we first discuss the form of the free energy functional.

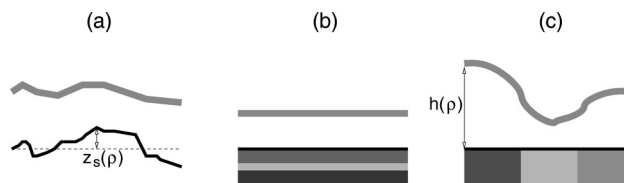If the membrane has an elastic modulus κ and tension σ,

FIG. 1. Supported membranes on structured surfaces. In (a), the membrane is adhering to a rough but otherwise homogeneous surface. The reference $\boldsymbol{\rho}$ plane is shown as a dashed line. The height of the lower membrane lipid leaflet and the surface, measured from this plane, are denoted by $h(\boldsymbol{\rho})$ and $z_s(\boldsymbol{\rho})$, respectively. Layered and columnar chemical structure are sketched in (b) and (c), respectively.

then its bending energy can be described by the functional [11]

$$\int dS \sqrt{g} \left[\sigma + \frac{1}{2} \kappa (2H)^2 \right], \qquad (2.1)$$

where the integral is over the membrane surface, g is the determinant of the metric, $H = (c_1 + c_2)/2$ the mean curvature, and c_1 and c_2 the two principal curvatures. We have ignored here the Gaussian curvature contribution as only a membrane with a fixed topology (flat on large length scales and of infinite size) is considered [12]. Throughout the paper we choose to work in the Monge representation. Letting $\boldsymbol{\rho} = (x, y)$ be a two-dimensional planar vector, the heights of the surface and membrane above some reference $\boldsymbol{\rho}$ plane are $z_s(\boldsymbol{\rho})$ and $h(\boldsymbol{\rho})$, respectively (see Fig. 1).

To account for the interaction of the membrane with the substrate, we include a potential term $V(h; z_s, \epsilon)$ in the free energy. As already mentioned, $z_s(\boldsymbol{\rho})$ accounts for the substrate's geometrical structure and describes its surface configuration, while $\epsilon(\mathbf{r})$ denotes any chemical inhomogeneities. The potential can have a number of different components [13,14]. For our case, the most important of these is the Van der Waals contribution, which is given by

$$V_{\text{vdw}}(h; z_s, \epsilon) = -[W(h; z_s, \epsilon) - W(h + \delta; z_s, \epsilon)], \quad (2.2)$$

where δ is the membrane thickness and is typically around 40 Å . Due to the bilayer nature of the membrane, two terms involving the Van der Waals potential $W(h; z_s, \epsilon)$ are necessary; in particular for supported membranes where $\delta \approx h$.

For a thin fluid film of thickness $h(\boldsymbol{\rho})$ resting on an inhomogeneous solid, one can sum over all possible pair interactions between the molecules in the upper half space, capped from below by the membrane surface $z = h(\boldsymbol{\rho})$, and those in the lower half space, capped from above by $z = z_s(\boldsymbol{\rho})$, to show that $W(h; z_s)$ satisfies [10]

$$W(h; z_s, \epsilon) = \int_{h(\boldsymbol{\rho})}^{\infty} dz \int d^2 \boldsymbol{\rho}' \int_{-\infty}^{z_s(\boldsymbol{\rho}')} dz' w_0(\mathbf{r} - \mathbf{r}')[1 + \epsilon(\mathbf{r}')]$$

$$(2.3)$$

with

$$w_0(\mathbf{r}) = \frac{A_0}{\pi^2} \left(\frac{1}{r^6} \right). \qquad (2.4)$$

The latter models nonretarded Van der Waals interactions. Equation (2.3) contains a position dependent Hamaker constant

$$A(\mathbf{r}) = A_0 [1 + \epsilon(\mathbf{r})] \qquad (2.5)$$

with A_0 the average value

$$A_0 = \frac{\int d^2 \mathbf{r} \, A(\mathbf{r})}{\int d^2 \mathbf{r}} \qquad (2.6)$$

and ϵ the (small) deviation around this average

$$\epsilon(\mathbf{r}) = \frac{A(\mathbf{r}) - A_0}{A_0}. \qquad (2.7)$$

We emphasize that $W(h; z_s, \epsilon)$ is a functional of both $z_s(\boldsymbol{\rho})$ and $\epsilon(\mathbf{r})$.

If $h(\boldsymbol{\rho})$ is set to a constant value, say h_0, and both z_s and ϵ vanish, then Eq. (2.3) becomes the familiar

$$W(h_0; 0, 0) \equiv W_0(h_0) = \frac{A_0}{12\pi} \cdot \frac{1}{h_0^2} \qquad (2.8)$$

(see Ref. [14]), which is just the Van der Waals potential between two planar semi-infinite bodies held a distance h_0 apart.

Equation (2.3) provides an attractive interaction and, for the case of a supported membrane, this is chiefly balanced by hydration forces. The hydration potential obeys

$$V_{\text{hyd}}(h; z_s) = b e^{-\alpha(h - z_s)}, \qquad (2.9)$$

where b has units of surface tension and α is an inverse length of typical size $\alpha^{-1} \simeq 2$–3 Å. Due to the very short range nature of the hydration interaction, we include the dependence on the substrate structure with a simple local approximation and so V_{hyd} is just a function of the local height $h(\boldsymbol{\rho}) - z_s(\boldsymbol{\rho})$. The origin of hydration forces is still under debate [14] but they are generally believed to have some steric contribution. Consequently, while b in general is position dependent we believe that this is a relatively minor effect and so choose to keep the simple form of Eq. (2.9).

The total potential is then

$$V(h; z_s, \epsilon) = V_{\text{vdw}}(h; z_s, \epsilon) + V_{\text{hyd}}(h; z_s) \qquad (2.10)$$

though one could consider more complicated scenarios involving, for example, electrostatic forces. Summing all these contributions we can write the total free energy as

$$\mathcal{F}[h] = \int d^2 \boldsymbol{\rho} \left\{ \sqrt{1 + (\nabla h)^2} \left[\sigma + \frac{\kappa}{2} \left(\vec{\nabla} \cdot \frac{\vec{\nabla} h}{\sqrt{1 + (\nabla h)^2}} \right)^2 \right] \right.$$

$$\left. + V(h; z_s, \epsilon) \right\}, \qquad (2.11)$$

where we have explicitly written out the curvature and tension terms in the Monge representation.

One of the most relevant quantities in experiments is the membrane adhesion energy. Within our general mean-field approach, the optimal height of the membrane is that which minimizes Eq. (2.11) and the value of the free energy when the membrane takes up this optimum configuration $\mathcal{F}_{\text{min}}$ leads to a natural definition of the adhesion energy per unit area

$$U \equiv - \left(\frac{\mathcal{F}_{\text{min}}}{S_0} - \sigma \right). \qquad (2.12)$$

TABLE I. The various parameters chosen and calculated for a supported membrane. For definitions, see text.

$\kappa = 35T$	$\sigma = 1.7 \times 10^{-5}$ J m^{-2}	$\delta = 38$ Å	$T = 4.1 \times 10^{-21}$ J
$A_0 = 2.6 \times 10^{-21}$ J	$b = 0.93$ J m^{-2}	$\alpha^{-1} = 2.2$ Å	
$a \simeq 49.3$ Å	$h_0 \simeq 0.61a \simeq 30$ Å	$U_0 \simeq 0.298\sigma$	$v \simeq 22.85a^{-2}\sigma$
$\xi_\sigma \simeq 0.21a$	$\xi_\kappa \simeq 1.97a$	$\xi \simeq 18.62a$	$\mathcal{V} \approx 1.30$

Here, S_0 is the total area of the projected reference ρ-plane, $S_0 = \int d^2\rho$ and we have subtracted off a membrane tension term. Doing so conveniently defines the adhesion energy so that a completely flat membrane does not have a tension dependent contribution; for a membrane infinitely far from the surface U will then vanish. Notice that Eq. (2.12) implies that an attractive surface will have a positive adhesion energy.

III. PLANAR AND HOMOGENEOUS SUBSTRATES

Our results are obtained by analytically expanding the free energy around its value taken for a planar, chemically homogeneous substrate. Therefore, we briefly review the results for such an ideal surface.

For this case, $\epsilon = z_s = 0$, and the Van der Waals interaction (2.3) simplifies to Eq. (2.8), and so

$$V_{\mathrm{vdw}}(h;0,0) = -[W_0(h) - W_0(h+\delta)], \qquad (3.1)$$

where throughout we use the subscript zero to denote adhesion at both chemically homogeneous and flat substrates. Here, a is a fundamental length scale in our problem

$$a = \left(\frac{A_0}{2\pi\sigma}\right)^{1/2} \qquad (3.2)$$

and is provided by the ratio of the Hamaker constant, see Eq. (2.8), and the membrane tension [15].

We find that the membrane adopts a flat configuration $h(\boldsymbol{\rho}) = h_0$, which obeys

$$\frac{\partial V}{\partial h} = V'_{\mathrm{vdw}}(h_0) - \alpha b e^{-\alpha h_0} = 0 \qquad (3.3)$$

from Eq. (2.9). The adhesion energy in this case is simply given as the negative of the interaction potential. From Eq. (2.11), $\mathcal{F}_{\min} = S_0[\sigma + V(h_0;0,0)]$ and so Eq. (2.12) implies that

$$U_0 = -V(h_0;0,0) = -[V_{\mathrm{vdw}}(h_0) + be^{-\alpha h_0}]. \qquad (3.4)$$

By definition, U_0 is positive for all sufficiently attractive potentials, V. Equations (3.3) and (3.4) provide the fundamental quantities upon which our perturbation theory will be built.

In order to allow (semiquantitative) comparison with experiment and to give some idea of the magnitude of the quantities involved, we would now like to specialize to a particular choice of our model parameters (we opt again for those chosen in Ref. [9]), see Table I. Typical experimental values of σ and κ are 1.7×10^{-5} J m^{-2} and $35T$, respec-

tively [16]. We set the Boltzmann constant to unity and so at room temperature $T = 4.1 \times 10^{-21}$ J. Choosing $A_0 = 2.6 \times 10^{-21}$ J $\simeq 0.63T$ [16], implies that the length scale $a \simeq 49.3$ Å and, from Eq. (3.3), $h_0 \simeq 0.61a \simeq 30$ Å in agreement with measured values using specular reflection of neutrons [17]. The two parameters used here to specify the hydration force, see Eq. (2.9), are

$$b = 0.93 \text{ J m}^{-2}; \quad \alpha^{-1} = 2.2 \text{ Å} \qquad (3.5)$$

which are in accordance with those measured in Ref. [18].

The potential experienced by the membrane, Eq. (2.10), is sketched in Fig. 2. From Eq. (3.4), one can see that

$$U_0 \simeq 0.298\sigma = 5.07 \times 10^{-6} \text{ J m}^{-2}. \qquad (3.6)$$

At this point, it is also worth discussing the other length scales which will appear in our treatment. Defining v as the second derivative of the potential calculated at the minimum $h = h_0$

$$v = \frac{\partial^2}{\partial h^2} V(h;0,0)\Bigg|_{h=h_0} = V''_{\mathrm{vdw}}(h_0;0,0) + V''_{\mathrm{hyd}}(h_0) \qquad (3.7)$$

several correlation lengths can be extracted,

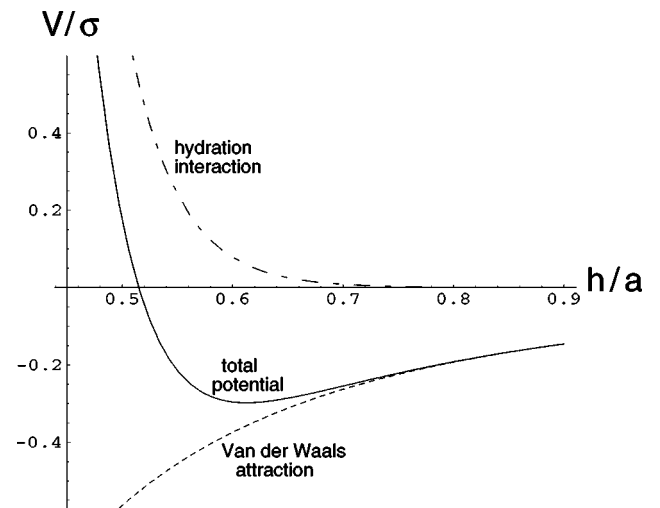$$\xi_\sigma^2 = \sigma/v, \quad \xi_\kappa^4 = \kappa/v \qquad (3.8)$$

FIG. 2. A plot of the various interactions described in Sec. III, with parameter values given in Table I. Here all potentials are measured in units of the membrane tension, $\sigma = 1.7 \times 10^{-5}$ J m^{-2}, and lengths in terms of $a \simeq 49.3$ Å. The total potential has a minimum at $h_0 \simeq 0.6a$.

together with

$$\xi^2 = \kappa/\sigma = \xi_\kappa^4 \xi_\sigma^{-2} \tag{3.9}$$

which describes the crossover between the tension and the rigidity dominated regimes. Their values for the experimental scenario described above are given in Table I (which also lists all the other model parameters).

IV. LINEAR RESPONSE THEORY

To carry out a perturbation theory for rough and heterogeneous substrates, we assume that z_s and $h - h_0$ are small, i.e., $z_s \sim h - h_0 \ll h_0$, and that any of their products and derivatives are also small. A (functional) Taylor expansion is then performed which is a fairly standard, if long, calculation.

To simplify our presentation and ease the algebra, we will assume that the chemical structure is such that ϵ can be factorized, i.e.,

$$\epsilon(\mathbf{r}) = \phi(\boldsymbol{\rho}) g(z) \tag{4.1}$$

for some functions ϕ and g and the substrate surface is given by $z_s = 0$. Such a factorization while including the layered (constant ϕ) and columnar (constant g) structures shown in Fig. 1 does prevent us from considering surfaces which are both rough and chemically inhomogeneous. Consequently from this point on, we will specialize to either rough or chemically patterned substrates.

A few more definitions are in order; first of all, we notice that v, given by Eq. (3.7), can also be shown to obey

$$v = V_{\text{hyd}}''(h_0) - \int d^2\boldsymbol{\rho}' \{ w_0(\boldsymbol{\rho}', h_0) - w_0(\boldsymbol{\rho}', h_0 + \delta) \} \tag{4.2}$$

using Eqs. (2.2) and (2.3). The kernel functions (this choice of nomenclature will become clear later)

$$K(\boldsymbol{\rho}) = -\frac{1}{v} [w_0(\boldsymbol{\rho}, h_0) - w_0(\boldsymbol{\rho}, h_0 + \delta)] \tag{4.3}$$

and

$$G(\boldsymbol{\rho}) = -\frac{1}{v} \int_{h_0}^{h_0 + \delta} dz \, g(h_0 - z) w_0(\boldsymbol{\rho}, z) \tag{4.4}$$

will also prove useful.

Then, expanding $\mathcal{F}[h]$ in Eq. (2.11) to second order and taking advantage of Eq. (3.3), we find

$$\frac{1}{\sigma}\mathcal{F} \approx \frac{1}{\sigma}\mathcal{F}_0 + \frac{1}{2\xi_\sigma^2} \int d^2\boldsymbol{\rho} \left\{ \xi_\sigma^2 (\nabla h)^2 + \xi_\kappa^4 (\nabla^2 h)^2 + (h - h_0)^2 \right.$$
$$\left. -2(h - h_0) \left[\mathcal{V} z_s + \int d^2\boldsymbol{\rho}' K(\boldsymbol{\rho}') z_s(\boldsymbol{\rho} + \boldsymbol{\rho}') \right] + z_s^2(\boldsymbol{\rho}) \right\} \tag{4.5}$$

for rough surfaces and

$$\frac{1}{\sigma}\mathcal{F} \approx \frac{1}{\sigma}\mathcal{F}_0 + \frac{1}{2\xi_\sigma^2} \int d^2\boldsymbol{\rho} \left\{ \xi_\sigma^2 (\nabla h)^2 + \xi_\kappa^4 (\nabla^2 h)^2 + (h - h_0)^2 \right.$$
$$\left. -2(h - h_0) \left[\int d^2\boldsymbol{\rho}' G(\boldsymbol{\rho}') \phi(\boldsymbol{\rho} + \boldsymbol{\rho}') \right] \right\} \tag{4.6}$$

for chemical patterning, where $\mathcal{F}_0 \equiv \mathcal{F}[h_0]$ is the h-independent term in the expansion,

$$\mathcal{F}_0 = \sigma \left[1 - \frac{1}{\sigma} U_0 \right] S_0. \tag{4.7}$$

In the case of chemical patterning, $\mathcal{F}_0$ contains an additional term

$$\int_{-\infty}^{0} dz V_{\text{vdw}}'(h_0 - z) \int d^2\boldsymbol{\rho}\, \epsilon(\boldsymbol{\rho}, z) \tag{4.8}$$

which vanishes if

$$\int d^2\boldsymbol{\rho}\, \phi(\boldsymbol{\rho}) = 0 \tag{4.9}$$

(an assumption we adopt for algebraic simplicity in some of the later formulas but certainly not a necessity). For rough substrates the $\boldsymbol{\rho}$ plane can be chosen so that $\langle z_s \rangle = \int d^2\boldsymbol{\rho}\, z_s = 0$. Here, $\mathcal{V}$ is given by

$$\mathcal{V} = \frac{V_{\text{hyd}}''(h_0)}{v}. \tag{4.10}$$

To find the optimum profile, we need to minimize Eq. (4.5) or (4.6) with respect to $h(\boldsymbol{\rho})$, i.e., $\delta\mathcal{F}/\delta h = 0$. The resulting Euler-Lagrange equation is nonlocal in $\boldsymbol{\rho}$ but linear in h,

$$[\xi_\kappa^4 \nabla^4 - \xi_\sigma^2 \nabla^2 + 1](h(\boldsymbol{\rho}) - h_0)$$
$$= \begin{cases} \int d^2\boldsymbol{\rho}' [K(\boldsymbol{\rho}' - \boldsymbol{\rho}) z_s(\boldsymbol{\rho}')] + \mathcal{V} z_s(\boldsymbol{\rho}), & \text{rough,} \\ \int d^2\boldsymbol{\rho}' [G(\boldsymbol{\rho}' - \boldsymbol{\rho}) \phi(\boldsymbol{\rho}')], & \text{chemical,} \end{cases} \tag{4.11}$$

where the role that K and G play as kernel functions becomes clear. Equation (4.11) is the starting point for our linear response profiles. It is a fourth order nonhomogeneous linear differential equation where the heterogeneity of the substrate enters in the nonhomogeneous term. Due to its linear nature, the solution can be written down in Fourier space. Defining for any function $f(\boldsymbol{\rho})$ its Fourier transform

$$\tilde{f}(\mathbf{q}) = \int d^2\boldsymbol{\rho} f(\boldsymbol{\rho}) e^{-i\mathbf{q}\cdot\boldsymbol{\rho}} \tag{4.12}$$

we find, via the convolution theorem, that $\delta h(\boldsymbol{\rho}) = h(\boldsymbol{\rho}) - h_0$ obeys

$$\delta\widetilde{h}(\mathbf{q})=\begin{cases}\dfrac{[\widetilde{K}(\mathbf{q})+\mathcal{V}]\widetilde{z}_s(\mathbf{q})}{1+\xi_\sigma^2q^2+\xi_\kappa^4q^4}, & \text{rough,}\\[14pt]\dfrac{\widetilde{G}(\mathbf{q})\widetilde{\phi}(\mathbf{q})}{1+\xi_\sigma^2q^2+\xi_\kappa^4q^4}, & \text{chemical.}\end{cases}\quad(4.13)$$

The Fourier transform $\widetilde{K}(\mathbf{q})$ of the kernel function $K(\boldsymbol{\rho})$ can be calculated using the result

$$\int d^2\boldsymbol{\rho}\,\frac{e^{-i\mathbf{q}\cdot\boldsymbol{\rho}}}{(\rho^2+h^2)^{m+1}}=2\pi\left(\frac{q}{2h}\right)^m\frac{K_m(qh)}{\Gamma(m+1)},\quad(4.14)$$

where $K_m(x)$ is the modified Bessel function of the second kind of order m. Nonretarded Van der Waals interactions are obtained by setting $m=2$ in the above equation [from Eq. (2.4)]. Then the kernel becomes

$$\widetilde{K}(\mathbf{q})=\widetilde{K}(q)=-\frac{\xi_\sigma^2q^2a^2}{2}\left[\frac{K_2(qh_0)}{h_0^2}-\frac{K_2(qh_0+q\,\delta)}{(h_0+\delta)^2}\right].$$

$$(4.15)$$

Notice that in the limit of q tending to zero, $\lim_{q\to0}q^2K_2(q)=2$, which implies that

$$\widetilde{K}(0)=-\xi_\sigma^2a^2\left(\frac{1}{h_0^4}-\frac{1}{(h_0+\delta)^4}\right)=1-\mathcal{V}\quad(4.16)$$

from Eqs. (3.7) and (4.10).

Similarly, $\widetilde{G}(\mathbf{q})$ satisfies

$$\widetilde{G}(\mathbf{q})=\widetilde{G}(q)=-\frac{\xi_\sigma^2a^2q^2}{2}\int_{h_0}^{h_0+\delta}dz\,\frac{g(h_0-z)}{z^2}K_2(qz)$$

$$(4.17)$$

which then implies that

$$\widetilde{G}(0)=-\xi_\sigma^2a^2\int_{h_0}^{h_0+\delta}dz\frac{g(h_0-z)}{z^4}.\quad(4.18)$$

For the case when $g(z)\equiv1$ (a columnar solid)

$$\widetilde{G}(0)=-\frac{\xi_\sigma^2a^2}{3}\left(\frac{1}{h_0^3}-\frac{1}{(h_0+\delta)^3}\right)<0\quad(4.19)$$

which will be needed in Sec. VI.

We can also calculate the adhesion energy in Fourier space by Fourier transforming Eq. (4.5). Using the solution of the Euler-Lagrange equation (4.13) and the definition of the adhesion energy, Eq. (2.12), then gives,

$$\frac{U}{\sigma}=\begin{cases}\dfrac{U_0}{\sigma}-\dfrac{1}{2S_0}\displaystyle\int\frac{d^2\mathbf{q}}{(2\pi\xi_\sigma)^2}\left(|\widetilde{z}_s(\mathbf{q})|^2-\dfrac{|(\widetilde{K}(\mathbf{q})+\mathcal{V})\widetilde{z}_s(\mathbf{q})|^2}{1+q^2\xi_\sigma^2+q^4\xi_\kappa^4}\right), & \text{rough}\\[18pt]\dfrac{U_0}{\sigma}+\dfrac{1}{2S_0}\displaystyle\int\frac{d^2\mathbf{q}}{(2\pi\xi_\sigma)^2}\left(\dfrac{|\widetilde{G}(\mathbf{q})\widetilde{\phi}(\mathbf{q})|^2}{1+q^2\xi_\sigma^2+q^4\xi_\kappa^4}\right), & \text{chemical.}\end{cases}\quad(4.20)$$

V. THE DERYAGIN APPROXIMATION

In a previous paper [9], we looked quite extensively at the adsorption of membranes on rough substrates and throughout used a Deryagin-like local approximation [19]. In this section we would like to show how this is included in our present, more general, linear response approach.

The Van der Waals potential (2.2) due to its functional (nonlocal) dependence on the inhomogeneities, provides most of the difficulties in any analytical method. These complications are neatly circumvented by the Deryagin approximation. Equation (2.3) can, by a simple change of variable, be rewritten as

$$W(h;z_s,\boldsymbol{\epsilon})=\begin{cases}\displaystyle\int_{h(\boldsymbol{\rho})}^\infty dz\int d^2\boldsymbol{\rho}'\int_{-\infty}^{z_s(\boldsymbol{\rho}+\boldsymbol{\rho}')}dz'\,w_0(\boldsymbol{\rho}',z-z'), & \text{rough,}\\[18pt]\displaystyle\int_{h(\boldsymbol{\rho})}^\infty dz\int d^2\boldsymbol{\rho}'\int_{-\infty}^0 dz'\,w_0(\boldsymbol{\rho}',z-z')[1+\phi(\boldsymbol{\rho}+\boldsymbol{\rho}')g(z')], & \text{chemical,}\end{cases}\quad(5.1)$$

where we have adopted Eq. (4.1). The Deryagin method amounts to replacing

$$z_s(\boldsymbol{\rho}+\boldsymbol{\rho}')\to z_s(\boldsymbol{\rho}),\quad\text{rough,}$$

$$(5.2)$$

$$\phi(\boldsymbol{\rho}+\boldsymbol{\rho}')\to\phi(\boldsymbol{\rho}),\quad\text{chemical,}$$

which removes the functional character of Eq. (5.1) and so neglects almost all nonlocal effects [we still retain the integral over $g(z')$]. Once Eq. (5.2) has been performed, one can (Taylor) expand the free energy in powers of $h-h_0$ and z_s as before.

However, such an approach turns out to be equivalent to replacing the kernel functions (4.3) and (4.4), in the linear

response theory by Dirac delta functions

$$K(\boldsymbol{\rho}-\boldsymbol{\rho}')\rightarrow\widetilde{K}(0)\,\delta(\boldsymbol{\rho}-\boldsymbol{\rho}'),$$

$$G(\boldsymbol{\rho}-\boldsymbol{\rho}')\rightarrow\widetilde{G}(0)\,\delta(\boldsymbol{\rho}-\boldsymbol{\rho}') \tag{5.3}$$

which transparently shows the local character of the Deryagin technique. Equation (5.3) implies that the Fourier transforms of the kernel functions are now simply constants.

Consequently, the Euler-Lagrange equation (4.11) becomes

$$(\xi_\kappa^4\nabla^4-\xi_\sigma^2\nabla^2+1)\,\delta h(\boldsymbol{\rho})=\begin{cases} z_s(\boldsymbol{\rho}), & \text{rough} \\ \widetilde{G}(0)\,\phi(\boldsymbol{\rho}), & \text{chemical,} \end{cases} \tag{5.4}$$

where we have used Eq. (4.16). In Fourier space the solution is

$$\delta\widetilde{h}(\mathbf{q})=\begin{cases} \dfrac{\widetilde{z}_s(\mathbf{q})}{1+\xi_\sigma^2 q^2+\xi_\kappa^4 q^4}, & \text{rough} \\[4mm] \dfrac{\widetilde{G}(0)\,\widetilde{\phi}(\mathbf{q})}{1+\xi_\sigma^2 q^2+\xi_\kappa^4 q^4}, & \text{chemical,} \end{cases} \tag{5.5}$$

with an adhesion energy given by Eq. (4.20) with the substitution (5.3),

$$\frac{U}{\sigma}=\begin{cases} \dfrac{U_0}{\sigma}-\dfrac{1}{2S_0}\displaystyle\int\dfrac{d^2\mathbf{q}}{(2\pi\xi_\sigma)^2}\left(\dfrac{(q^2\xi_\sigma^2+q^4\xi_\kappa^4)|\widetilde{z}_s(\mathbf{q})|^2}{1+q^2\xi_\sigma^2+q^4\xi_\kappa^4}\right), & \text{rough} \\[5mm] \dfrac{U_0}{\sigma}+\dfrac{1}{2S_0}\displaystyle\int\dfrac{d^2\mathbf{q}}{(2\pi\xi_\sigma)^2}\left(\dfrac{|\widetilde{G}(0)\,\widetilde{\phi}(\mathbf{q})|^2}{1+q^2\xi_\sigma^2+q^4\xi_\kappa^4}\right), & \text{chemical.} \end{cases} \tag{5.6}$$

For the case of roughness, these are exactly the results obtained in our previous paper [9]. We note that there is a difference in sign between the two cases; while $\delta U\equiv U-U_0<0$ for the rough case, $\delta U>0$ for chemically patterned surfaces. This is one of our main observations and will be discussed in Sec. VI C.

It is also possible to indicate the regime where the Deryagin approximation can be expected to be valid. Using the observation that this approximation is recovered in the zero wave number limit [see (5.3)] and assuming that the structure, be it chemical or geometrical, is dominated by one long wavelength mode such that $qa\ll 1$, then comparing the zeroth and second order terms in an expansion of Eq. (4.13) to order $(qa)^2$ implies that

$$\frac{q^2\xi_\sigma^2 a^2}{4}\left(\frac{1}{h_0^2}-\frac{1}{(h_0+\delta)^2}\right)\ll 1 \tag{5.7}$$

for rough surfaces and

$$\frac{q^2}{4}\int_{h_0}^{h_0+\delta}\frac{g(h-z)}{z^2}dz\ll\int_{h_0}^{h_0+\delta}\frac{g(h-z)}{z^4}dz \tag{5.8}$$

for chemical inhomogeneities, which becomes

$$\frac{q^2}{4}\left[\frac{1}{h_0}-\frac{1}{h_0+\delta}\right]\ll\left[\frac{1}{h_0^3}-\frac{1}{(h_0+\delta)^3}\right] \tag{5.9}$$

when $g(z)\equiv 1$. If these conditions are violated (providing $qa\ll 1$) then a Deryagin approach will fail though we stress that Eqs. (5.7) and (5.8) while necessary for the validity of the Deryagin approximation are certainly not sufficient.

Shifting our interest momentarily away from supported membranes, if we allow $h_0\gg\delta$, then Eq. (5.7) and (5.8) simplify considerably and become $\xi_\sigma\ll h_0$ and $h_0\ll a$, respectively.

VI. PREDICTIONS OF THE LINEAR RESPONSE METHOD

The nonlocal perturbation method is embodied by Eqs. (4.11) and (4.20). In this section we compare and contrast this approach with the simpler local Deryagin approximation. As both methods are based on perturbation theory, we have the caveat that

$$\frac{\delta U}{U_0}\ll 1 \tag{6.1}$$

for the method to be valid, i.e., that the perturbation correction is much smaller than the term it improves on. The fundamental difference between the approaches is in the treatment of the Van der Waals potential; in the Deryagin approximation there is only a purely local attraction while the linear response includes non-local collective effects. The Euler-Lagrange equations (4.11) and (5.4) most clearly illustrate this.

A. Chemically structured surfaces

For the types of structure considered, Eq. (4.5) gives the general linear response free energy. One can define a bending (BE) and potential energy (PE) contribution to this by simply letting the bending energy be that part which vanishes when σ and κ are set to zero and the potential energy that part that remains. Then, using the solution (4.13), we find
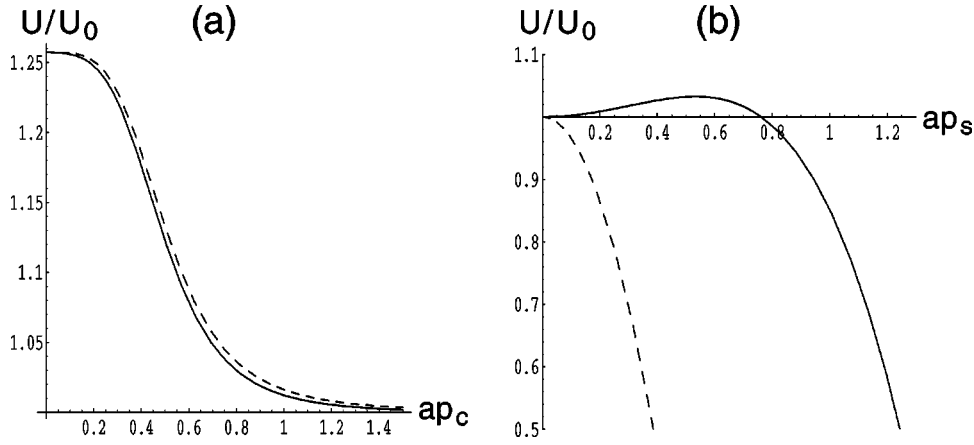
FIG. 3. Membrane adhesion energy for a substrate which (a) is flat and has a sinusoidally varying Hamaker constant ($\Lambda_c = 10.0$) and (b) has a sinusoidal surface configuration ($\Lambda_s = 2.0a$) plotted against wave number. The Deryagin solution is also shown with a dashed line.

$$PE_{chem} = -\int \frac{d^2\mathbf{q}}{(2\pi)^2} \frac{1+2Q}{(1+Q)^2} |\tilde{G}(\mathbf{q})\tilde{\phi}(\mathbf{q})|^2 \quad (6.2)$$

and

$$BE_{chem} = \int \frac{d^2\mathbf{q}}{(2\pi)^2} \frac{Q}{(1+Q)^2} |\tilde{G}(\mathbf{q})\tilde{\phi}(\mathbf{q})|^2 \quad (6.3)$$

with $Q = \xi_\sigma^2 q^2 + \xi_\kappa^4 q^4$ [a constant contribution, $V(h_0;0,0)$, has been ignored in the potential energy term]. Here and throughout the rest of the paper, we fix $g(z) \equiv 1$ for clarity and so consider only columnar solids. The reader interested in layered solids should consult Ref. [10] whose results can be simply extended to membranes.

Using the fact that

$$0 > \tilde{G}(q) \geqslant \tilde{G}(0) \quad (6.4)$$

for all q, and remembering that the Deryagin approximation is recovered when the kernel function $\tilde{G}(q)$ is set to its value at $q = 0$, one can see almost by inspection that the membrane potential energy will be higher than in the Deryagin case while the bending energy will be lower. In fact, the increment in the potential energy will be greater than the bending energy decrement and we can therefore expect the surface to appear less attractive, due to nonlocal effects, with a correspondingly lower U.

A sinusoidally patterned surface, translationally invariant in the y direction, is the simplest choice with which to illustrate this behavior. Setting

$$\phi(\boldsymbol{\rho}) = \Lambda_c \sin(p_c x) \quad (6.5)$$

with Λ_c being the amplitude of the Hamaker coefficient oscillations and $2\pi/p_c$ their period, Eq. (4.13) then implies

$$h(\rho) = h_0 + \frac{\Lambda_c \tilde{G}(p_c) \sin(p_c x)}{1 + \xi_\sigma^2 p_c^2 + \xi_\kappa^4 p_c^4}, \quad (6.6)$$

where $\tilde{G}(p_c) < 0$ from Eq. (6.4). The adhesion energy is also easily calculated

$$\frac{U}{\sigma} = \frac{U_0}{\sigma} + \frac{1}{4\xi_\sigma^2} \frac{\Lambda_c^2 |\tilde{G}(p_c)|^2}{1 + p_c^2 \xi_\sigma^2 + p_c^4 \xi_\kappa^4}. \quad (6.7)$$

In Fig. 3(a), this adhesion energy is plotted against wave number p_c. One can see that there is good agreement between the Deryagin and linear response approaches. As the period of the sinusoidal variation increases the membrane is less and less able to respond to the structural variations and for high p_c the adhesion energy takes its planar value once more. Any chemical structure has been effectively washed away.

B. Rough surfaces

In this case, the two contributions to the adhesion energy are

$$PE_{rough} = \int \frac{d^2\mathbf{q}}{(2\pi)^2} |\tilde{z}_s(\mathbf{q})|^2 \left\{ 1 - |\tilde{K}(\mathbf{q}) + \mathcal{V}|^2 \frac{1+2Q}{(1+Q)^2} \right\} \quad (6.8)$$

and

$$BE_{rough} = \int \frac{d^2\mathbf{q}}{(2\pi)^2} \frac{Q}{(1+Q)^2} |[\tilde{K}(\mathbf{q}) + \mathcal{V}] \tilde{z}_s(\mathbf{q})|^2. \quad (6.9)$$

As

$$\tilde{K}(q) + \mathcal{V} \geqslant \tilde{K}(0) + \mathcal{V} = 1 \quad (6.10)$$

for all q, the complete opposite behavior results with the bending energy increased by the nonlocal contributions and the potential energy decreased below the decrement to the bending energy. The surface becomes more attractive and the adhesion energy increases above the Deryagin result.

Looking at a chemically homogeneous but geometrically corrugated surface we choose

$$z_s(\boldsymbol{\rho}) = \Lambda_s \sin(p_s x) \quad (6.11)$$

so that the surface corrugations have an amplitude of Λ_s and a period of $2\pi/p_s$. Equation (4.13) gives

$$h(\boldsymbol{\rho}) = h_0 + \frac{\Lambda_s[\tilde{K}(p_s) + \mathcal{V}]\sin(p_s x)}{1 + \xi_\sigma^2 p_s^2 + \xi_\kappa^4 p_s^4} \qquad (6.12)$$

with $\tilde{K}(p_s) > 0$ from Eq. (6.10), while U obeys

$$\frac{U}{\sigma} = \frac{U_0}{\sigma} - \frac{\Lambda_s^2}{4\xi_\sigma^2}\left[1 - \frac{|\tilde{K}(p_s) + \mathcal{V}|^2}{1 + p_s^2\xi_\sigma^2 + p_s^4\xi_\kappa^4}\right]. \qquad (6.13)$$

This latter result is plotted in Fig. 3(b) and deviates substantially from the Deryagin prediction as p_s increases. Nonlocal effects are important and can strongly decrease the membrane potential energy. In particular, notice that for small p_s the adhesion energy is *increased* above the value taken for the planar situation. This can never occur in the Deryagin approximation [see Eq. (5.6) and Ref. [9]]. The additional Van der Waals contribution accounted for substantially raises the membrane potential energy. For large p_s, positive nonlocal effects "saturate," i.e., $\tilde{K}(p_s)$ plateaus, and U starts to decrease for greater p_s values, see Eq. (6.13). In general, the membrane finds it more difficult to adhere to the rough surface and the adhesion energy will asymptotically (large p_s) tend to a constant value less than unity (though for the high value of Λ_s chosen our perturbation theory is not sufficiently accurate to capture this). The membrane potential energy eventually becomes positive while its bending energy vanishes as $p_s \to \infty$.

Again, it is important to reiterate that our approach is strictly only valid when Eq. (6.1) holds.

C. Comparison between chemically structured and rough surfaces

Consider once more Eq. (4.13), with $Q = \xi_\sigma^2 q^2 + \xi_\kappa^4 q^4$,

$$\delta\tilde{h}(\mathbf{q}) = \begin{cases} \dfrac{[\tilde{K}(\mathbf{q}) + \mathcal{V}]\tilde{z}_s(\mathbf{q})}{1 + Q}, & \text{rough} \\[3mm] \dfrac{\tilde{G}(\mathbf{q})\tilde{\phi}(\mathbf{q})}{1 + Q}, & \text{chemical.} \end{cases} \qquad (6.14)$$

Two points are worth making. (i) From Eqs. (6.4) and (6.10) it can be seen that the membrane amplitude is increased and decreased by nonlocal effects for roughness and chemical structure, respectively. This is reflected in a corresponding change in the bending energy (compared to the Deryagin results). (ii) Due to the different signs of $\tilde{K} + \mathcal{V}$ and $\tilde{G}$, see Eqs. (6.4) and (6.10) again, the membrane profile is always in phase with the surface contour of a rough substrate but is exactly out of phase with surface structure arising due to chemical variation. A membrane adhering to a rough surface will, in order to maximize its potential energy, try and follow that surface as best it can (limited only by the resulting bending energy cost). Similarly, the membrane will follow the hills and valleys of a substrate potential generated by chemical patterning. In this case, however, a local increase or decrease in the Hamaker constant A makes that region of the surface more or less attractive and so shifts the membrane in
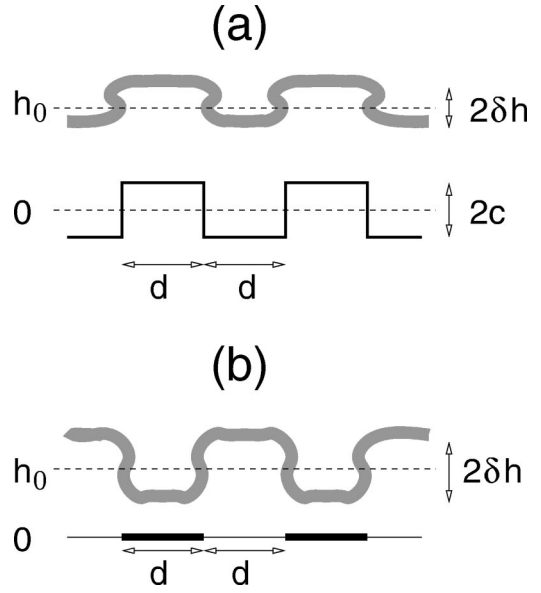

FIG. 4. A membrane adhering to (a) a substrate with a square wave surface configuration and (b) to a flat substrate periodically striped with two different chemical compounds.

or out. Note that the membrane would be in phase with the substrate for a repulsive Van der Waals potential [20].

By using the Deryagin approximation, simple arguments describing an effective potential energy highlight the different adhesive properties of the two surfaces. In Fig. 4, a surface (translationally invariant in the y direction) patterned with a square wave profile and a similar on/off chemical patchwork is schematically shown. For the former case, a definition for an effective potential energy is given by

$$V_{\text{eff}} = \frac{\displaystyle\int dx\, V(h - z_s)}{\displaystyle\int dx} \qquad (6.15)$$

which just equals $V(h_0)$ for the planar scenario $z_s = 0$. When the substrate is square corrugated this approximately becomes

$$V_{\text{eff}} \approx \frac{1}{2}\{V(h_0 + \delta h - c) + V(h_0 - \delta h + c)\}$$

$$= V(h_0) + \frac{1}{2}(\delta h - c)^2 V''(h_0) + O[(\delta h - c)^4]$$

$$> V(h_0) \qquad (6.16)$$

as $V''(h_0)$ is positive (h_0 being a minimum of V). Thus even in this crude argument, one can see that surface roughness acts (at least if the roughness does not get too large when our perturbation expansion breaks down) to increase the membrane potential energy—a result verified by the Deryagin version of Eq. (6.8). Equation (6.16) shows that surface roughness is reminiscent of Gaussian thermal fluctuations and similarly to these acts to drive the membrane out of its potential minimum.

When the wall is patterned with a periodic array of alternating chemical patches as in Fig. 4, one can use similar arguments to those given above to estimate the effective potential energy. Let the Hamaker constant A obey

$$A = \begin{cases} A_0(1+\phi), & \text{dark patch} \\ A_0(1-\phi), & \text{light patch,} \end{cases} \quad (6.17)$$

for constant and positive A_0 and ϕ, then the potential energy is, see Eqs. (2.5) and (2.10),

$$V(h) = V_{\text{vdw}}(h)\epsilon(x) + V_{\text{hyd}}(h) \quad (6.18)$$

with $\epsilon(x) = 1 \pm \phi$ on the dark and light patches. Therefore,

$$V_{\text{eff}} = \frac{\int dx\, V(h)}{\int dx}$$

$$= \frac{1}{2}\{V_{\text{vdw}}(h_0 - \delta h)(1+\phi) + V_{\text{hyd}}(h_0 - \delta h)$$

$$+ V_{\text{vdw}}(h_0 + \delta h)(1-\phi) + V_{\text{hyd}}(h_0 + \delta h)\}$$

$$= V(h_0) + \frac{1}{2}\delta h^2 V''(h_0) - \phi \delta h V'_{\text{vdw}}(h_0) + O(\delta h^3).$$

$$(6.19)$$

Notice here that the membrane's position is exactly out of phase with the surface structure. This leads to a negative contribution in Eq. (6.19) and one can see that the new membrane configuration, as the negative term is of order δh and positive is of order δh^2, is likely to result in a net attractive contribution to the potential energy. Indeed, this can be verified by summing Eqs. (6.2) and (6.3) which, as already mentioned, is always negative.

In summary, a membrane generally adheres less favorably (relative to the planar and homogeneous surface) to a rough substrate and adopts a configuration that is in phase with the surface contours. A chemically structured substrate has a higher adhesion energy (more favorable) and leads to a membrane configuration exactly out of phase with the surface structure.

VII. COMPARISON BETWEEN EXACT AND APPROXIMATE SOLUTIONS

From these examples and those given in Ref. [9], it is clear that the Deryagin approximation is certainly the most versatile if one wishes to obtain analytical results. However, it is also apparent that in some situations nonlocal effects can become important and in this section we compare the Deryagin result with an exact numerical solution.

The scenario we choose to specialize to involves solely geometric inhomogeneities. We consider a chemically pure substrate made up of a regular array (in the x direction) of "V" shaped trenches. These could be formed, for example, by etching silicon wafers [21]. In the other spatial dimension, i.e., the y direction, the system is translationally invariant.
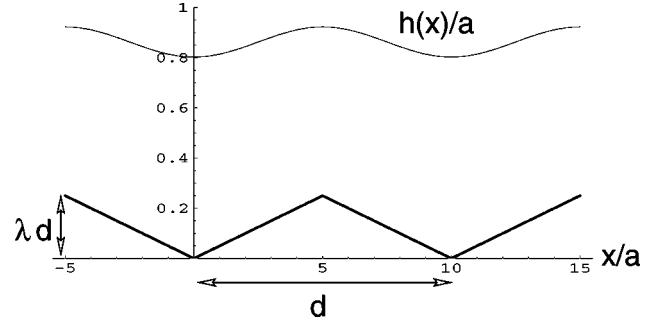

FIG. 5. A typical membrane configuration predicted by the Deryagin approximation for adsorption above a homogeneous substrate sculptured with "V"-shaped trenches. The parameters for a single trench are $d=10a$ and $\lambda=0.05$, which implies a width of around 500 Å and depth of approximately 25 Å. The adhesion energy is $U \approx 0.43 U_0$.

For simplicity, the trenches are assumed to be symmetric about their lowest point and have a maximum width of d and a depth of λd. See Fig. 5 for an example.

A. The Deryagin solution

To find the Deryagin solution it is most easy to consider Eq. (5.4) directly, which reduces to a one-dimensional differential equation. This is

$$\left(\xi_\kappa^4 \frac{d^4}{dx^4} - \xi_\sigma^2 \frac{d^2}{dx^2} + 1\right)\delta h(x) = z_s(x) \quad (7.1)$$

with

$$z_s(x) = 2\lambda \sum_{n=-\infty}^{\infty} \{r_x[\theta(x+nd) - \theta(x+nd-d/2)]$$

$$+ (d-r_x)[\theta(x+nd-d/2) - \theta(x+nd-d)]\}, \quad (7.2)$$

where $\theta(x)$ is the Heaviside function and $r_x = x \bmod d$, i.e., the remainder of x on division by d. Assuming that the membrane has the same symmetry as the substrate, the boundary conditions are

$$h'(nd) = h'''(nd) = 0,$$

$$h'(nd+d/2) = h'''(nd+d/2) = 0 \quad (7.3)$$

for all integers n.

Due to the periodicity of $z_s(x)$, we need only solve Eq. (7.1) for $0 < x < d/2$, where $z_s(x) = 2\lambda x$, and then reflect and/or translate this solution to obtain the full membrane configuration. We find in this region that for $\boldsymbol{\rho} = (x,y)$,

$$h(\boldsymbol{\rho}) = h_0 + 2\lambda x - \frac{2\lambda \eta_+^2 \eta_-^2}{\eta_+^2 - \eta_-^2}[\psi_+(x) - \psi_-(x)] \quad (7.4)$$

with

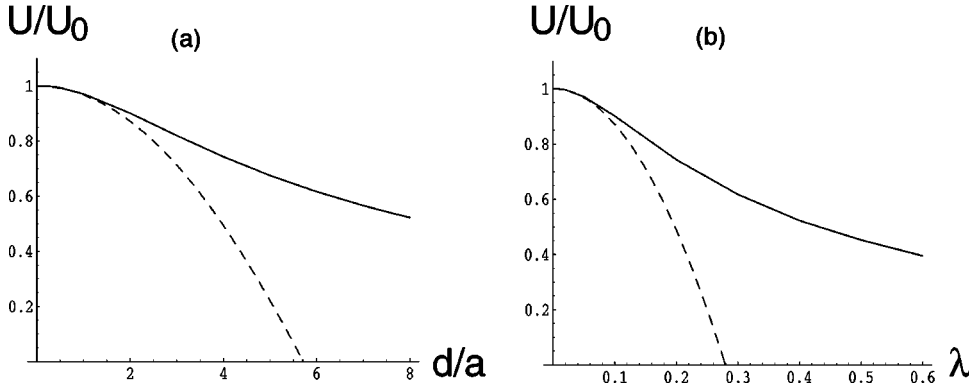$$\psi_\pm(x) = \frac{\sinh[(\frac{1}{4}d - x)\eta_\pm]}{\eta_\pm^3 \cosh(\frac{1}{4}\eta_\pm d)}. \quad (7.5)$$

FIG. 6. A comparison of the Deryagin predictions (dashed lines) and an exact numerical solution (heavy lines) for the adhesion energy U above a substrate patterned with "V" shaped trenches. In (a) U/U_0 is plotted as a function of d/a with $\lambda = 0.1$, while for (b), it is shown as a function of λ and $d = 2a$. For small d/a or λ the Deryagin method provides a good approximation to the numerical result.

The $\eta_{\pm}$ come from the factorization of the operator in Eq. (7.1), see Ref. [9], and are

$$\eta_{\pm} = \xi^{-1} \left[\frac{1 \pm \sqrt{1 - 4(\xi/\xi_{\kappa})^4}}{2} \right]^{1/2}, \qquad (7.6)$$

where ξ is given by Eq. (3.9). The height profile of the membrane, $h(x)$ is plotted in Fig. 5 using Eq. (7.4).

The adhesion energy is obtained from the definition (2.12). Equation (4.5) with Eq. (5.3) implies

$$\frac{U}{\sigma} = \frac{U_0}{\sigma} - \frac{1}{d} \int_0^{d/2} dx \{ h'^2 + \xi^2 h''^2 + \xi_{\sigma}^{-2} (h - h_0 - 2\lambda x)^2 \}. \qquad (7.7)$$

Using Eq. (7.4), the above integral can be calculated analytically yielding

$$\frac{U}{\sigma} = \frac{U_0}{\sigma} - 4\lambda^2 \left\{ \frac{1}{2} + \frac{I(d\eta_+, d\eta_-) + I(d\eta_-, d\eta_+)}{d^4(\eta_+^2 - \eta_-^2)^2} \right\} \qquad (7.8)$$

with

$$I(u,v) = \frac{2u(\xi/\xi_{\kappa})^4}{(\xi/d)^2} \left\{ \frac{4}{1 + e^{u/2}} - \frac{2[1 + 2(\xi/\xi_{\kappa})^2]}{(\xi/d)^2(u^2 - v^2)} \right.$$

$$\left. + \frac{(\xi/d)^2 v^2 (2u^2 - v^2)}{(\xi/\xi_{\kappa})^4 u^2} \tanh(\tfrac{1}{4}u) \right\}. \qquad (7.9)$$

Figure 6 (dashed lines) illustrates Eq. (7.8) and compares it with the exact numerical solution detailed below.

B. The exact numerical solution

In this subsection we present a numerical solution which accounts for the full Van der Waals interaction (2.2) and the bending energy term in Eq. (2.11). One can functionally minimize Eq. (2.11) but the resulting Euler-Lagrange equation is nonlinear and very complicated. Given that Eq. (7.2) implies the boundary conditions (7.3), the resulting problem is extremely awkward to tackle even numerically if one tries to solve the equation directly. Instead, we choose first to discretize Eq. (2.11) and then minimize the free energy func-

tional with respect to all of the discrete variables. This has the advantage that the boundary conditions (7.3) can be easily incorporated.

For one-dimensional structures, such as the trench geometry, (2.11) becomes

$$\mathcal{F}[h] = \int dx \left\{ \sigma \sqrt{1 + h'^2} + \frac{\kappa}{2} \frac{h''^2}{(1 + h'^2)^{5/2}} + V(h; z_s, 0) \right\}. \qquad (7.10)$$

Due to the symmetry of Eq. (7.2), we only need consider a solution for $0 < x < d/2$ and adopt a standard discretization process by dividing the interval, i.e.,

$$h'(x_k) \leftrightarrow \frac{h_{k+1} - h_k}{\Delta}, \qquad h''(x_k) \leftrightarrow \frac{h_{k+2} - 2h_{k+1} + h_k}{\Delta^2}, \qquad (7.11)$$

where $x_k = k\Delta$, $k = 1, \ldots, N$ and $\Delta = d/2N$. Here, N is the number of points making up the one-dimensional lattice and typically was chosen somewhere between 100 and 400. For the simple surface (7.2), Eq. (2.3) can be broken into a (convergent) infinite sum of integrals each of which can then be evaluated analytically.

Carrying out this procedure we find Figs. 6 and 7. From the adhesion energies plotted in Fig. 6, there is a region of good agreement between the Deryagin and exact solution. This agreement occurs for low d and λ where Eq. (6.1) holds. As the Deryagin approximation underestimates the attractive potential in this case, the adhesion energy is always less than the exact result and it is also reassuring that the exact U does not vanish for high d or λ. This prediction of the Deryagin approach is clearly an artifact of going beyond the limits of perturbation theory. Generally, we see that the adhesion energy decreases with greater values of the roughness, i.e., large λ or d (for small d any structure is effectively "washed out" and not seen by the membrane).

The degree of penetration of the membrane into the "V"-shaped trenches is shown in Fig. 7 where the membrane height above the middle of the trench, $\delta h(0) = h(0) - h_0$, is plotted. One can see that the membrane always lies further away from the substrate than if the latter were entirely planar and so there is no penetration into the surface indentations. However, this could be encouraged by having flat regions
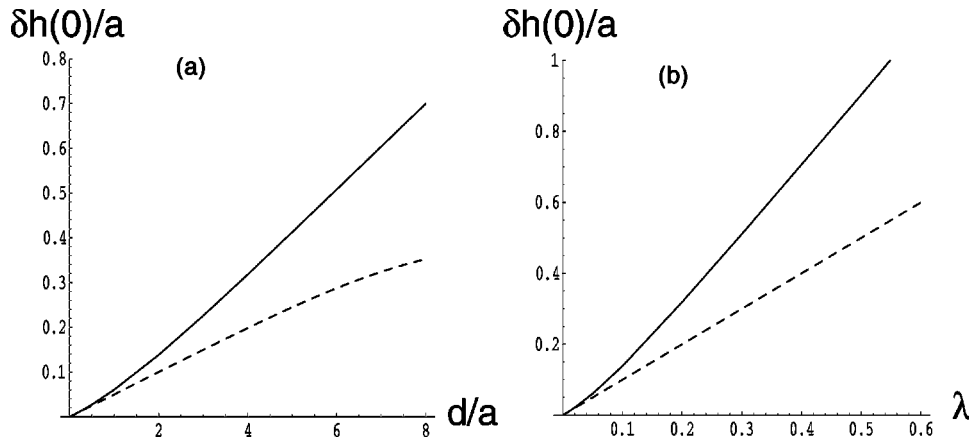
$\delta h(0)/a$ (a)

$\delta h(0)/a$ (b)

d/a

λ

FIG. 7. The membrane height in the center of a ''V'' shaped trench measured with respect to its planar height $\delta h(0)$ $= h(0) - h_0$. In (a) $\delta h(0)$ is plotted as a function of the trench width d/a while in (b) it is plotted as a function of the trench amplitude with $d = 2a$. The numerical solution (heavy line) soon departs from the Deryagin result (dashed line) with good agreement again only occurring for values of the adhesion energy close to U_0.

separating each trench (see Ref. [9] for a similar example). As the surface becomes rougher, it also becomes more repulsive (U decreases) and so the membrane moves outwards. It is perhaps surprising to see that the exact solution lies furthest away from the substrate despite having a higher adhesion energy. This is likely to be a consequence of higher order bending energy terms in Eq. (7.10) reducing the amplitude of the membrane configuration and so increasing its height at the center of a trench.

VIII. CONCLUSIONS

A significant experimental question is whether or not, compared to a planar, homogeneous surface, substrate structure encourages membrane adhesion. An important conclusion of our study is that columnar chemical structure [see Fig. 1(c)], which obeys Eq. (4.9), always increases a substrate's attractiveness; the membrane potential energy (6.2) is clearly negative and also greater than the bending energy (6.3). Consequently, the adhesion energy increases. Rough surfaces are unfortunately more ambiguous as Eq. (6.8) is not of a definite sign. However, if the Deryagin approximation is invoked [$\tilde{K}(q) + \mathcal{V} \approx 1$], then the potential energy contribution is always positive. Therefore, we would expect roughness to usually decrease a substrate's attractiveness and lead to a drop in the adhesion energy. We should emphasize that for surfaces for which nonlocal effects are important this may no longer be the case.

Some comments on the validity of our approach are also worth mentioning. Both analytical methods breakdown when the amplitude of the structure, be it geometrical or chemical, becomes large. This is to be expected as our analysis is fundamentally a perturbation method and can only be confidently followed when Eq. (6.1) holds. The linear response technique is an improvement over Deryagin and is particularly appropriate for rough surfaces where the additional nonlocal effects lead to an increase in the amplitude of an adhering membrane. For smoothly varying surfaces these effects can even lead to the surface becoming attractive—a result that is not predicted by the local Deryagin approximation. Unfortunately, it is difficult to identify the particular geometries for which nonlocal Van der Waals contributions are important but for those surfaces of biotechnological interest, i.e., with trenches or indentations etched into them, they do not seem to lead to radically different behavior. To conclude, if one wishes an analytical guide to how a certain substrate structure will influence membrane adhesion and if that structure can be conveniently described in Fourier space then the linear response description is the method of choice. Failing this the Deryagin approximation is quick and easy to apply if only normally adequate for small amplitude effects.

Throughout this paper we have looked only at generic chemical patterning described by a position dependent Hamaker constant. In the future, it will be of interest to extend this work to include particular chemical patterns and specific interactions between the membrane and the surface, such as a receptor ligand or an antigen antibody [22–24].

[1] E. Sackmann, Science **271**, 43 (1996); J. Rädler and E. Sackmann, Curr. Opin. Solid State Mater. Sci. **2**, 330 (1997).

[2] E. Sackmann, FEBS Lett. **346**, 3 (1994).

[3] J. Salafsky, J. T. Groves and S. G. Boxer, Biochemistry **35**, 14 773 (1996).

[4] A. T. A. Jenkins, R. J. Bushby, N. Boden, S. D. Evans, P. F. Knowles, Q. Liu, R. E. Miles, and S. D. Ogier, Langmuir **14**, 4675 (1998).

[5] J. T. Groves, N. Ulman, and S. G. Boxer, Science **275**, 651 (1997).

[6] T. D. Osborn and P. Yager, Langmuir **11**, 8 (1995).

[7] S. D. Ogier, R. J. Bushby, Y. Cheng, S. D. Evans, S. W. Evans, A. T. A. Jenkins, P. F. Knowles, and R. E. Miles, Langmuir **16**, 5696 (2000).

[8] U. Seifert and R. Lipowsky, Phys. Rev. A **42**, 4768 (1990); M. Kraus, U. Seifert, and R. Lipowsky, Europhys. Lett. **32**, 431 (1995).

[9] P. S. Swain and D. Andelman, Langmuir **15**, 8902 (1999).

[10] D. Andelman, J. F. Joanny, and M. O. Robbins, Europhys. Lett. **7**, 731 (1988); M. O. Robbins, D. Andelman, and J. F. Joanny, Phys. Rev. A **43**, 4344 (1991).

[11] P. B. Canham, J. Theor. Biol. **26**, 61 (1970); W. Helfrich, Z. Naturforsch. C **28**, 693 (1973).

[12] The Gauss-Bonnet theorem then implies that the Gaussian curvature contribution is constant and so can be safely neglected.

[13] R. Lipowsky, in *Structure and Dynamics of Membranes*, edited by R. Lipowsky and E. Sackmann (Elsevier, Amsterdam, 1995).

[14] J. N. Israelachvili, *Intermolecular and Surface Forces* (Academic Press, London, 1992).

[15] P. G. de Gennes, Rev. Mod. Phys. **57**, 827 (1985).

[16] J. O. Rädler, T. J. Feder, H. H. Strey, and E. Sackmann, Phys. Rev. E **51**, 4526 (1994).

[17] S. J. Johnson, T. M. Bayerl, D. C. McDermot, G. W. Adam, A. R. Rennie, R. K. Thomas, and E. Sackmann, Biophys. J. **59**, 289 (1991).

[18] K. Gawrisch, D. Ruston, J. Zimmerberg, V. A. Parsegian, R. P. Rand, and N. Fuller, Biophys. J. **61**, 1213 (1992).

[19] B. V. Deryagin, Kolloidn. Zh. **17**, 827 (1955); B. V. Deryagin, N. V. Churaev, and V. M. Muller, *Surface Forces* (Consultants Bureau, New York, 1987).

[20] Note that this is the usual wetting case where a negative Hamaker constant leads to a repulsive Van der Waals force—the disjoining pressure of Deryagin. In fact, to recover a wetting scenario in our equations one needs simply to take the limit of the membrane thickness δ going to infinity.

[21] S. Gerdes and G. Ström, Colloids Surf., A **116**, 135 (1996).

[22] R. Lipowsky, Phys. Rev. Lett. **77**, 1652 (1996).

[23] T. Weikl, R. R. Netz, and R. Lipowsky, Phys. Rev. E **62**, 45 (2000).

[24] S. Komura and D. Andelman, Eur. Phys. J. E **3**, 259 (2000).